

A dynamical mean-field study of rare-earth nickelates

D. Misra¹, N. S. Vidhyadhiraja², and A. Taraphder^{1,3}

¹Department of Physics, Indian Institute of Technology Kharagpur, Kharagpur, India

²Theoretical Sciences Unit, Jawaharlal Nehru Centre For Advanced Scientific Research, Jakkur, Bangalore, India

³Centre for Theoretical Studies, Indian Institute of Technology Kharagpur, Kharagpur, India

E-mail: debolina@phy.iitkgp.ernet.in

Abstract.

Most of the rare-earth Nickelates (RNiO₃; R= Nd, Pr, Sm etc.) exhibit a sharp metal-insulator transition, from a high temperature paramagnetic metal to a low temperature antiferromagnetic insulator. LaNiO₃, the first member of the series, is the only exception in the RNiO₃ family, which remains metallic down to low temperatures. Using local density approximation as an input to dynamical mean-field theory, we study the transport properties of both LaNiO₃ and NdNiO₃, and show that LaNiO₃ remains a correlated Fermi liquid with an effective mass enhancement as the correlation increases upto the bandwidth. We also suggest the possibility of pressure and strain-driven metal-insulator transition in both the Nickelate compounds.

1. Introduction

Considerable experimental and theoretical knowhow has been brought to bear upon the problem of rare-earth Nickelate series (RNiO₃, R=La, Nd, Pr etc) over the past two decades to come to grips with their unusual structural and electronic properties across the series. In the series RNiO₃, all the members except LaNiO₃ are insulators at low temperatures [1, 2]. They (R≠La) undergo a sharp transition from a high temperature paramagnetic metal (PMM) to a low temperature antiferromagnetic insulator (AFI) at characteristic temperatures T_{MI} , which increase with the radii of the rare earth atoms [3]. The magnetic and resistive transitions are coupled in NdNiO₃ and PrNiO₃ ($T_{MI}=T_N$, the Neel temperature), whereas for the other Nickelates, $T_{MI} > T_N$. While NdNiO₃ is an antiferromagnetic insulator at low temperature, LaNiO₃ is the only exception in the series, remaining a paramagnetic metal down to lowest temperatures measured, never undergoing a metal-insulator transition(MIT) [1, 2, 3]. The reason behind the different ground states of two very similar compounds is still under active investigation[4, 5]. Apart from the ground state properties, LaNiO₃ differs from NdNiO₃ from the structural point of view also; while LaNiO₃ is rhombohedral, NdNiO₃ has an orthorhombic structure. The MIT seen in Nickelates is structurally correlated with the crystal tolerance factor t_r which measures the deviation of the crystal structure from an ideal cubic one, and is given by $t_r = \frac{d_{R-O}}{\sqrt{2}d_{Ni-O}}$.

While LaNiO₃ has an ideal cubic structure with the largest bandwidth (W) among the 3d transition metal Nickelates, others have smaller bandwidths due primarily to their distorted structures [1]. As we move from La, Pr, Nd to Eu and Y, the radius of the rare-earth



atom decreases, and the NiO₆ octahedron tilts to accommodate the mismatch in the unit cell parameters. The tilting is minimum, and hence the tolerance factor t_r is maximum for the first few Nickelates (La, Nd, Pr), indicating that the structural distortion has little effect on their electronic properties. On the other hand, for the RE ions with smaller radii, the distortion is maximum and plays a key role behind the MIT they undergo. We intend to provide a theoretical account for the metallic ground state and transport properties of LaNiO₃ using local density approximation (LDA) as an input to a dynamical mean field theory (DMFT). We also comment on the next member NdNiO₃ and argue that the MIT there cannot only come from correlation, the change in structure and charge order are essential to understand the MIT as the bandwidth reduces.

2. Methods and formalism

The small structural distortion in both LaNiO₃ and NdNiO₃ ($t_r \approx 0.97$ and 0.94 , respectively) allows one to adopt a pseudo-cubic notation to study their electronic structures. An LCAO (linear combination of atomic orbitals) band-structure calculation for the LDA density of states is performed for LaNiO₃, and a tight binding fit is obtained using Wannier90 for the two LDA bands (e_g^*) obtained from WIEN2K [6], that straddle the Fermi level (FL). In the cubic structure the rare-earth atoms (R=La,Nd) sit at the corner, Ni atoms at the body-center, and the O atoms at the face-center positions. In RNiO₃ compounds, the nominal electronic configuration is Ni d^7 , with fully filled triply degenerate t_{2g} orbitals and quarter-filled 2-fold degenerate e_g orbitals. However, there is considerable controversy on the exact filling [7], values quoted ranging from 6.78 to 8.2 electrons in the 3d bands. Coming from a face-to-face overlap of two atomic orbitals, σ bonds are the strongest covalent bonds, while π bonds are much weaker due to a side-by-side overlap. This prompted consideration of only σ bonding [3, 5] between Ni 3d and its nearest O 2p orbitals. Two Ni e_g orbitals ($d_{x^2-y^2}$ and $d_{3z^2-r^2}$) and three O 2p orbitals (p_x, p_y, p_z along the respective axes) therefore constitute a 5x5 Hamiltonian which in turn gives five bands. Out of these five, two e_g^* antibonding bands formed out of hybridization between Ni 3d and O 2p orbitals and degenerate along the Γ -R direction cross the Fermi level. Bandwidths for these bands came out to be of the order of Coulomb energy (U_{dd}) for the Nickelate series, implying a moderately correlated situation.

An LCAO fit to the e_g^* bands and the corresponding density of states (DOS) were obtained using Wannier90 routine [6]. This LCAO DOS for the two e_g^* bands were taken as the input for our DMFT calculations using multi-orbital iterated perturbation theory (MO-IPT) as the impurity solver. DMFT is considered to be one of the most accurate techniques to study correlated systems, as it takes full account of the temporal fluctuations, while IPT, which uses the second order term in the perturbative expansion in U , is already shown to produce very good results at considerably less numerical cost. In the presence of a residual hybridization between the two e_g^* bands, the filling in each band is not conserved separately and the physics is influenced by the inter-band exchange and spectral weight transfer over large energy ranges. The paramagnetic phase of LaNiO₃ is, therefore, well described by the two-band Hamiltonian

$$\mathcal{H} = - \sum_{\langle ij, \mu, \nu \rangle, \sigma} t_{ij, \mu, \nu} (c_{i\sigma, \mu}^\dagger c_{j\sigma, \nu} + h.c.) + U \sum_{i, \mu} n_{i\uparrow, \mu} n_{i\downarrow, \mu} + U' \sum_{i, \mu, \nu, \mu \neq \nu} n_{i, \mu} n_{i, \nu} \quad (1)$$

Here $t_{ij, \mu, \nu}$ is the hopping between nearest neighbour sites i and j across the bands μ, ν , $c_{i\sigma, \mu}^\dagger$ ($c_{i\sigma, \mu}$) is the creation (annihilation) operator for an electron of spin σ in orbital μ ($= 1, 2$) at the i -th site. These orbitals represent the two e_g^* orbitals from LCAO fit and U, U' are the on-site intra- and inter-band Coulomb repulsions respectively. Typical values of correlation, used for the entire d-band width in LaNiO₃ is about 7 eV [7], little less than the total d-bandwidth. For

only the e_g^* part of the band, use of this value of U would be more than twice the e_g^* bandwidth and clearly unrealistic. An effective correlation U , of upto the same order of the e_g^* bandwidth is therefore reasonable. The LDA e_g^* band DOS (Fig.1) shows that almost the entire weight of the DOS is contained within a range of about 3 eV, which, would then be the upper limit for the correlations appropriate for the calculations that follow.

The essential idea of DMFT is to replace the many-body lattice model by a single site impurity problem, embedded in a bath, determined self-consistently [8]. This works exactly in infinite dimensions, while being a local approximation in finite dimensions, it captures the temporal fluctuations over a large scale very effectively. This is marked by the emergence of a low energy coherence scale in the DMFT as correlation increases, a feature missed by almost all other theories. The non-interacting DOS is the input of our DMFT calculations for the local retarded Green's function $G(\omega) = \mathcal{H}[\gamma(\omega)]$, where $\gamma = \omega + i\eta - \Sigma(\omega)$ and $\mathcal{H}(z)$ is the Hilbert transform of ρ_0 , given by

$$\mathcal{H}(z) = \int d\epsilon \frac{\rho_0(\epsilon)}{z - \epsilon} \quad (2)$$

The self-consistency condition in DMFT demands that the lattice self-energy be same as the impurity one and hence the self-energy is local. The one-electron Greens function ($G_a(\omega)$) and the associated self-energy ($\Sigma_a(\omega)$) for any orbital a, are related to the bath propagator ($\mathcal{G}_a(\omega)$) via Dyson's equation

$$\mathcal{G}_a^{-1}(\omega) = G_a^{-1}(\omega) + \Sigma_a(\omega) \quad (3)$$

The self-energy $\Sigma_a(\omega)$ is calculated within MO-IPT and is given by

$$\Sigma_a(\omega) = \frac{\sum_b A_{ab} \Sigma_{ab}^{(2)}}{1 - \sum_b B_{ab} \Sigma_{ab}^{(2)}} \quad (4)$$

$$\Sigma_{ab}^{(2)}(\omega) = 2 \frac{U_{ab}^2}{\beta^2} \sum_{m,n} \mathcal{G}_a(i\omega_m) \mathcal{G}_b(i\omega_n) \mathcal{G}_b(i\omega_m + i\omega_n - i\omega) \quad (5)$$

Where $\Sigma_{ab}^{(2)}(\omega)$ is the second order contribution to the self-energy, A_{ab} and B_{ab} are the necessary coefficients [9], a and b denote the two different orbitals, and $i\omega_m$ and $i\omega_n$ are the Matsubara frequencies. From the imaginary frequency spectral function following the analytical continuation: $i\omega_n \rightarrow \omega + i\eta$, the Matsubara summation is then carried out. The bath propagator is given by,

$$\mathcal{G}_a(\omega) = \frac{1}{\omega + \mu_a - \Delta_a(\omega)} \quad (6)$$

where $\Delta_a(\omega)$ is the dynamical Weiss field for orbital a[9]. From the imaginary part of self-energy, the real part is calculated by the Kramers-Kronig transformation [8].

Transport properties can be calculated fairly accurately within the single band DMFT, owing to the cancellation of vertex corrections in the corresponding Kubo formula. However, this does not apply in the multi-band situation and one has to neglect the vertex corrections as they are generally known to be small. However, being a convolution of two Green's functions and from two bands in this case, transport is a difficult calculation inherently. These results and their consequences are discussed in detail elsewhere[10].

3. Results and analysis

The spectral functions at different correlations U were calculated for LaNiO_3 and are shown in Fig.1: It is evident from Fig.1 that for upto the interaction strengths of U , U' about 2.0 eV and 1.0 eV respectively, there is no real gap in the DOS at the Fermi level for LaNiO_3 rendering it metallic down to lowest temperatures. Both the bands have non-zero spectral weight at the Fermi level. What is important is the transfer of spectral weight to high energies (upto 3 eV and more). Although the transfer is not too much in terms of weight, the range is quite large for the values of correlation we work with. The situation is very similar for NdNiO_3 as well [10], confirming the general assertion [1] that the lattice distortions and charge ordering play a crucial role in the formation of the insulating state in NdNiO_3 .

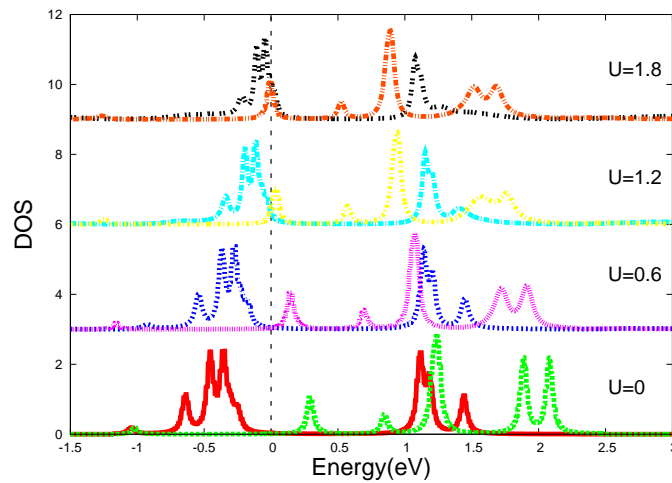


Figure 1. Evolution of density of states with energy for LaNiO_3 , as U increases. The red, blue, cyan and black lines denote the lower e_g^* band at different correlation U , while the green, pink, yellow and orange lines are for the upper e_g^* band. The spectral weight transfer and persistent non-zero DOS at FL is notable.

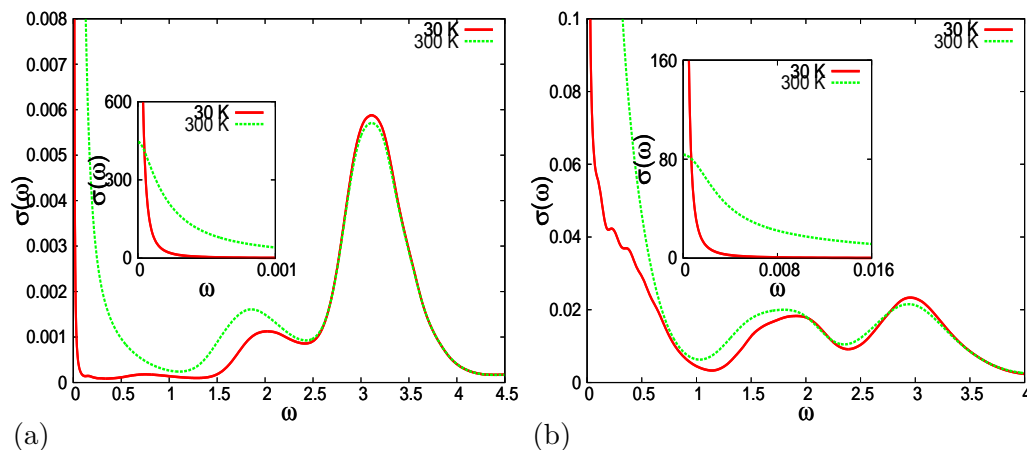


Figure 2. Optical conductivity $\sigma(\omega)$ as a function of ω (in eV) for (a) $U=0.6$ eV and (b) $U=1.8$ eV respectively. The red (continuous) and green (dashed) lines are for temperatures 30 and 300 K. The inset shows the recovery of spectral weight at low temperatures in the nearly divergent Drude peak at very low energies.

The real and imaginary parts of the self-energy were calculated for different values of U . While $\Sigma(\omega)$ varies quadratically with ω close to FL [11] even for a moderate U , a typical signature of the correlated metallic state, it becomes linear at higher frequency. No pole in $\text{Im}\Sigma(\omega \rightarrow 0)$ is observed in any band indicating the absence of orbital selective transitions here as well. The correlated metallic state has a reasonable mass enhancement at the lower band, extracted from the quasiparticle residue at the FL, of about 2 for $U=2.0$ eV and increasing with U , though much lower than what is observed in the experiments.

Optical conductivity in both the systems LaNiO_3 and NdNiO_3 show very unique features connected to Mott physics [12, 13]. The optical conductivity is calculated in the MO-DMFT and we observe clear signature of correlation as shown in the changing sharpness of the Drude peaks with change in temperature (Fig.2). From Fig. 2(main panel) it seems that the spectral weight is transferred to the lower energy region with increase in temperature, while a careful study of the optical conductivity spectra reveals that the weight is actually recovered in the vicinity of zero energy region, as shown in the insets of Fig. 2. For the lower U value, the peaks appearing near 1.7 eV and 3 eV are possibly due to the inter-band transitions, while the enhanced weight of the 1.7 eV peak for the moderately strong correlation ($U=1.8$ eV) indicates the formation of Hubbard sub-bands, and owes its origin to the inter Hubbard-band transitions. There is no strong evidence of phonon in the infrared region of the optical conductivity spectra [12].

Thin films of both the systems, grown on different substrates, show quite interesting strain dependence. While it is evident that strain certainly has effects on T_{MI} , however, whether the sign of strain really affects the nature of transition or not, is not clear. Several reports dealing with the effect of strain on MIT of Nickelates seem to contradict each other and vary widely. For example, in 30 uc LaNiO_3 films, it appears, that both tensile and compressive strains cause increased coherence [12]. Usually one would expect opposite behaviours in the two cases. The effect of strain on T_{MI} of Nickelates is actually not straight-forward, as strain can not be decoupled from oxygen vacancy, which in turn changes the resistivity of the system under consideration. In the context of our calculations, an increase (decrease) in t/U ratio is expected with compressive (tensile) strain leading to an increase (decrease) of coherence.

In summary, we have calculated the spectral and transport properties of LaNiO_3 using MO-DMFT. Our calculations clearly reveal LaNiO_3 as a Fermi liquid; albeit correlated, which never undergoes a Mott transition. While LaNiO_3 has the maximum bandwidth, and hence the minimum U/W ratio, it increases as we move from La to Nd, Pr etc, thereby favouring the insulating state over the metallic one eventually. However, without incorporating the structural distortion and charge-ordering, we find [10] that NdNiO_3 follows almost similar progression of DOS and transport as shown for LaNiO_3 above. It is, therefore, essential that one would have to include these inputs (as well as magnetism) to model systems beyond LaNiO_3 in the Nickelate series.

4. Acknowledgement

We acknowledge help at various stages of the work from Swagata Acharya, Monodeep Chakrabarti and Tulika Maitra. Research of DM was supported by a fellowship from IIT Kharapur, India.

5. References

- [1] Catalan G 2008 *Phase Transitions* **81** 729.
- [2] Medarde M 1997 *J. Phys.: Condens. Matter* **9** 1679.
- [3] Hamada N, 1993 *J. Phys.: Chem. Solids* **54** 1157.
- [4] Misra D, 2014 *Phase Trans.* **87** 398.
- [5] Lee S B, Chen Ru and Balents Leon, 2011 *Phys. Rev. B* **84** 165119.
- [6] Blaha P, *et al.*, WIEN2K, An Augmented Plane Wave+ Local Orbitals Program for Calculating Crystal Properties, edited by K. Schwarz, Technische Universitat Wien, Austria, 2001.

- [7] Park H, et al., 2014 arxiv:1409.4135.
- [8] Georges A, et al. 1996 *Rev. Mod. Phys.* **68** 13.
- [9] Laad M S, Craco L, and Mller-Hartmann E, 2006 *Phys. Rev. B* **73** 045109.
- [10] Misra D, et al., to be published.
- [11] Misra D, 2014 arXiv:1401.7133v2
- [12] Stewart M K, et al., 2011 *Phys. Rev. B* **83** 075125.
- [13] Stewart M K, et al., 2011 *Phys. Rev. Lett* **107** 176401.